Chemosphere 332 (2023) 138844

Contents lists available at ScienceDirect

Chemosphere

journal homepage: www.elsevier.com/locate/chemosphere

Partitioning of heavy metals in sediments and microplastics from stormwater runoff

Amali Herath [a], Dibya Kanti Datta [b], Gholamreza Bonyadinejad [a], Maryam Salehi [b,*]

[a] Department of Civil Engineering, The University of Memphis, Memphis, TN, USA
[b] Department of Civil and Environmental Engineering, The University of Missouri, Columbia, MO, USA

HIGHLIGHTS

- UV photodegradation increased the uptake of Cu, Zn, and Pb by MPs.
- Photodegradation enhanced the leaching of dissolved organic carbon from MPs.
- The presence of photodegraded MPs reduced the metal uptake by sediments.
- The second-order kinetic model described the metal uptake by MPs and sediments.

GRAPHICAL ABSTRACT

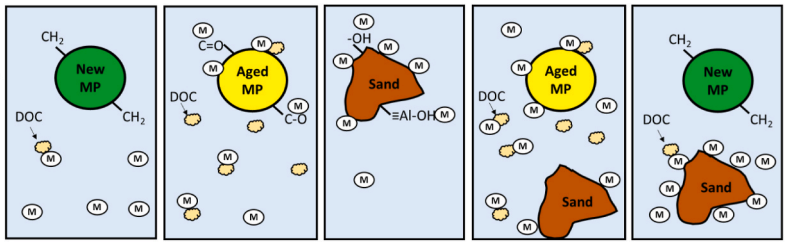

ARTICLE INFO

Handling Editor: Michael Bank

Keywords:
Stormwater
Heavy metals
Microplastics
Microstructure
Photodegradation
Runoff

ABSTRACT

Microplastics could act as vehicles for transporting heavy metals from urban environments to water resources via stormwater runoff. Although the transport of heavy metals by sediments has been widely studied, there is a lack of mechanistic understanding of their competition with microplastics (MPs) for heavy metal uptake. Therefore, this study was conducted to examine the partitioning of heavy metals in microplastics and sediments from stormwater runoff. For this purpose, new low density polyethylene (LDPE) pellets were selected as representative MPs, and accelerated UV-B irradiation experiments were conducted for eight weeks to generate photodegraded MPs. The competition of Cu, Zn, and Pb species for the occupation of available surface sites on sediments and new and photodegraded LDPE MPs was examined through 48 h kinetics experiments. Additionally, leaching experiments were conducted to identify the extent of organics released into the contact water by new and photodegraded MPs. Moreover, 24 h metal exposure experiments were conducted to identify the role of initial metal concentrations on their accumulation onto the MPs and sediments. The photodegradation process altered the LDPE MPs' surface chemistry by creating the oxidized carbon functional groups [>C═O, >C–*O*–C<], and it also enhanced their dissolved organic carbon (DOC) leaching into the contact water. The results showed significantly greater levels of Cu, Zn, and Pb accumulations on photodegraded MPs compared to the new MPs in either absence or presence of sediments. Heavy metal uptake by sediments when photodegraded MPs were present was significantly reduced. This might be due to the organic matter leached by photodegraded MPs into the contact water.

* Corresponding author.
E-mail addresses: mshfp@missouri.edu, msalehiesf@gmail.com (M. Salehi).

https://doi.org/10.1016/j.chemosphere.2023.138844
Received 23 February 2023; Received in revised form 30 April 2023; Accepted 2 May 2023
Available online 6 May 2023

1. Introduction

Heavy metals (HMs) are considered to be the primary pollutants present in urban environment (Jahandari, 2020). They are generated by natural processes and anthropogenic activities within the urban areas. Abundance of commonly found HMs [e.g., Zn, Cu, Pb, Cd, Ni] varies by population density, type of industrial activities [e.g., power plants, coal combustion], and traffic emission [e.g., vehicle exhaust, tire wear particles] (Kamali et al., 2023). Despite significant efforts dedicated to exploring the spatial variations of HMs in stormwater and urban dust (Fiala and Hwang, 2021; Salehi et al., 2020), less attention has been paid to their accumulation onto and transport by other suspended solids, such as plastic particles that are present within the urban sediments. Global plastic consumption has increased due to its pleasing features, such as low cost, flexibility, durability, lightweight, and corrosion resistance (Zhang et al., 2021). It's estimated that more than 8300 million metric tons of plastics produced since the early 1900s have been dumped into landfilled or left within the environment (Geyer et al., 2017).

By maintaining similar plastic production rates and waste management practices, it is projected that by 2050, approximately 12,000 million metric tons of plastic waste will accumulate within landfills and the environment (Geyer et al., 2017). The critical impacts of plastics on ecology and human health are not limited to their persistent nature and chemical leaching [flame retardant, plasticizers] (Kitahara and Nakata, 2020) but also to their ability to transport contaminants such as HMs, pathogens, and organics to the adjacent water resources (Gao et al., 2021; Scott et al., 2021). The major drivers of plastic pollution within the urban environment include littering, tire wear particles, road marking, atmospheric fallout, and improper solid waste management (Rødland et al., 2022). Exposure of plastic residuals to biological, mechanical, and physiochemical factors results in their conversion to smaller particles known as microplastics (MPs). Stormwater runoff is a significant pathway for MPs [1.1 to 24.6 particles/L] to reach aquatic habitats (Werbowski et al., 2021). Therefore, it is essential to understand how MPs interact with other contaminants present in stormwater runoff to evaluate their contaminant transport behavior. We have recently reported that abrasion of low density polyethylene (LDPE) and polyethylene terephthalate (PET) MPs with sediments results in silt accumulation onto their surface, which increases their Pb and Zn uptake. Subsequent exposure of the metal-accumulated MPs to the synthetic stormwater at pH = 5.0 resulted in the Zn and Pb release to the contact water, which occurred at a greater rate for the new MPs than for weathered MPs (Aghilinasrollahabadi et al., 2021). We also underscored the critical role of plastics' intrinsic properties, such as molecular structure and orientation, in their photodegradation behavior, where a greater polymeric crystallinity promoted both LDPE and HDPE UV stability (Herath and Salehi, 2022).

Heavy metals that are present in stormwater runoff can attach to suspended solids because of their larger surface areas and greater cation exchange capacities (Herngren et al., 2005). It's estimated that more than 90% of the total HMs found in urban waterways accumulate onto sediments, posing a relatively low risk to the aquatic environment (Miranda et al., 2022). On the other hand, the enhanced surface polarity of MPs due to the weathering may result in their increased metal accumulation (Huang et al., 2020; Hadiuzzaman et al., 2022). Variations in water chemistry, such as pH, could result in the desorption of accumulated HMs, thus, increasing their bioavailability (Aghilinasrollahabadi et al., 2021; Ahamed et al., 2020).

In recent years, metal accumulation onto MPs has been well investigated in the marine environment; however, less attention has been paid to metal uptake by MPs in stormwater, despite stormwater being a major route for transporting MPs to both fresh and marine environments. Furthermore, information regarding the partitioning of HMs between MPs and sediment is lacking despite the abundance of sediment within stormwater runoff. This critical information is needed to better assess the risk of MPs to ecology and also to evaluate the extent of HMs transport via sediment and MPs transport processes. The lower density of MPs with respect to sediments enhances their mobility and thus increases the risk of HMs transport from the urban environment to the surrounding water resources. Therefore, it is imperative to investigate the HM uptake characteristics of MPs in stormwater. Thus, this study aims to elucidate the Pb, Zn, and Cu partitioning between new and photodegraded LDPE MPs and the sediments present in the stormwater. Moreover, it provides an understanding of the alterations of MPs' surface chemistry and dissolved organic carbon (DOC) leaching characteristics due to the accelerated photodegradation process. The null hypotheses in this study are as follows: (i) there is no difference in metal uptake between new and photodegraded MPs, and (ii) there are no impacts caused by new and photodegraded MPs on heavy metals uptake by sediments present in stormwater.

2. Experimental

2.1. Materials

In this study, new (as received from the manufacturer) low density polyethylene (LDPE) pellets (r = 1.77 mm) were used as the model MPs (Figure S1). They were purchased from Sigma Aldrich and had a melt index of 25 g/10 min. ICP-MS standards for Cu^{2+}, Zn^{2+}, and Pb^{2+} (1000 mg/L in 3% nitric acid) were purchased from RICCA chemical company. The water used to create the synthetic stormwater was treated with Ultrapure Milli-Q (18 MΩ*cm). Sand was used as the representative of the sediments for the experiments, and its size distribution is presented in Table S1. Before conducting metal uptake experiments, the sand was pyrolyzed at 500 °C for 4 h in a muffle furnace to eliminate its organic components and exclude the impact of soil organic content on metal uptake results.

2.2. Accelerated photodegradation experiments and MPs' characterization

The new LDPE MPs were placed in the open glass Petri dishes and exposed to UV-B radiation in a Q-UV accelerated weathering tester (The Q-panel Company, Cleveland, OH, USA) at a constant intensity of 1.25 $mWcm^{-2}$. The UV-B lamps irradiated at wavelengths of 280–315 nm. The photodegradation experiments were conducted for 8 weeks at 50 °C. LDPE MPs were evenly placed in Petri dishes for uniform exposure to UV-B radiation. The MPs were randomly mixed every four days for uniform exposure to UV-B irradiation (Herath and Salehi, 2022; Hadiuzzaman et al., 2022; Bonyadinejad et al., 2022). Surface chemistry characterization was conducted for new and UV-B exposed MPs using Attenuated Total Reflectance Fourier Transformed Infrared Spectroscopy (ATR-FTIR). For this purpose, the ATR-FTIR spectra were recorded using a Thermoscientific ATR-FTIR spectrophotometer from 4000 to 400 cm^{-1} with a 4 cm^{-1} resolution. The degree of plastic photodegradation was evaluated by calculating the Carbonyl Index (CI) according to equation (1), where A_{1723} and A_{2870} are the absorbances of carbonyl and methylene bonds, respectively (Salehi et al., 2018; Babaghayou et al., 2016).

$$CI = A_{1723} / A_{2870} \quad (1)$$

The Brunauer–Emmett–Teller (BET) model was used to determine the surface area. An ASAP2020 analyzer from the Micromeritics Instrument Corp. Was used to measure MPs' BET surface area. About 100 mg of MPs was initially degassed at 70 °C for 15 h under vacuum (less than 5 μm Hg) before analysis. Nitrogen gas adsorption isotherms were obtained for the MPs from the relative pressure of 10 μm Hg to 760 mm Hg at 77.5 K. Surface area of the samples wascalculated using the BET equation.

2.3. Dissolved organic carbon (DOC) leaching experiments

DOC leaching experiments were conducted to identify the extent of organic carbon leached from new and photodegraded LDPE MPs into the contact water. For this purpose, 300 mg of unrinsed new and photodegraded LDPE pellets were added to 24 mL of synthetic stormwater with a pH of 7.0, and shaken using an orbital shaker at 200 rpm at 25 °C. Water samples were collected at different time intervals [2 h, 12 h, 24 h, 48 h, 120 h], filtered using 0.45 μm glass fiber syringe filters, and stored in airtight glass vials at 4 °C prior to the analysis. Duplicate samples were collected, and their DOC concentrations were quantified using Shimadzu TOC VCPN total organic carbon analyzer. The calibration curve for the analysis was developed using standard solutions of 0, 5, 10, and 20 mg/L DOC, and the R^2 value for the calibration curve was 0.9999. Samples over the concentration of 20 mg/L were diluted ten times using Millipore-treated water before analysis. The detection limit for measurement of DOC concentration was 0.2 mg/L. The chemical composition of synthetic stormwater used for these experiments is shown in Table S2.

2.4. Heavy metal exposure experiments

In this study, a series of metal exposure experiments were conducted to examine the partitioning of HMs between MPs and sediments. Cu^{2+}, Zn^{2+}, and Pb^{2+} were selected for the HM exposure experiments due to their persistence in urban storm runoff (Salehi et al., 2020; Herngren et al., 2005). Synthetic stormwater (Table S2) was used for HM exposure experiments. LDPE MPs (300 mg) were added into polypropylene tubes with 24 mL of an aqueous solution containing a mixture of Cu, Zn, and Pb. Initially, the metal accumulation onto the new and photodegraded MPs was compared by conducting metal exposures for 6 h and 12 h using initial concentrations of 300 μg/L at pH = 7.0 in the absence of sediments. Similar experiments were conducted only for sediments at three different concentrations of 200 mg/L, 400 mg/L, and 600 mg/L, which correspond to the addition of 4.8, 9.6, and 14.4 mg of sediments to aqueous samples (24 mL), respectively. Then, kinetics experiments were conducted for five different systems containing (a) only new MPs, (b) only photodegraded MPs, (c) only sediments, (d) new MPs and sediments, and (e) photodegraded MPs and sediments, as summarized in Table 1. All metal exposure experiments were performed in triplicate. The polypropylene tubes containing new and photodegraded LDPE MPs were shaken using an orbital shaker at 200 rpm at room temperature. The samples were filtered using Whatman filter paper (No. 1) at intervals of 2, 6, 12, 24, and 48 h, and the sediments were separated from the LDPE MPs. After the metal exposure experiments, the plastic pellets were digested in 2% HNO_3 acid (10 mL) for 24 h, the remaining filtrate was acidified with 2% HNO_3 acid, and the tubes were rinsed with 2% HNO_3 acid (10 mL). The Cu, Zn, and Pb concentrations were analyzed using an Inductively Coupled Plasma Optical Emission Spectrometer (ICP-OES, Varian 710-ES). Calibration curves for all metal ions were constructed from 1 to 300 μg/L. The limit of detection (LOD) for Cu^{2+}, Zn^{2+}, and Pb^{2+} was calculated as 3.1, 3.9, and 4.9 μg/L, respectively.

This study examined the metal adsorption onto the new and photodegraded MPs and sediment particles using first and second-order kinetics models. Moreover, the influence of HMs' initial concentrations on the rate of accumulation onto the MPs and sediments was examined via 24 h metal exposure experiments. Batch sorption experiments were conducted for five different systems, including the new and photodegraded MPs, and sediments, similar to the kinetics experiments. The initial concentrations of Cu^{2+}, Zn^{2+}, and Pb^{2+} varied from 100 μg/L to 2000 μg/L in synthetic stormwater at pH 7.0. The extent of metal uptake by sediments in the aqueous mixture of MPs and sediments was determined by applying the mass balance equation as shown in equation (2), in which M_{sed} is the mass of metal accumulated by the sediments, M_t is the total mass of metal present in the system, M_{aq} is the total metal present in the aqueous phase after metal exposure experiments, M_{MPs} is the mass of metal accumulated onto the MPs, and M_{tube} is the mass of metal quantified in the tubes' rinsate.

$$M_{sed} = M_t - \left(M_{aq} + M_{MPs} + M_{tube}\right) \quad (2)$$

Adherence of sediment particles to the surface of MPs during the metal exposure experiments was a challenge. To address this, after removing the MPs from the solution, they were rinsed with a small volume of synthetic stormwater with similar pH to the aqueous solution. The student *t*-test was performed to identify the significant difference in HM uptake and organic leaching by new and photodegraded MPs. Statistical significance was determined with a 95% corresponding confidence interval.

Table 1
Experimental conditions for the kinetics experiments.

Condition / Parameter	(a)	(b)	(c)	(d)	(e)
Type of MPs	New	Photodegraded	None	New	Photodegraded
MPs mass (mg)	300	300	0	300	300
Sediment (mg/L)	0	0	200	200	200
Cu^{2+} (μg/L)	500	500	500	500	500
Zn^{2+} (μg/L)	500	500	500	500	500
Pb^{2+} (μg/L)	500	500	500	500	500

3. Results and discussion

3.1. Heavy metals speciation

The speciation of Pb^{2+}, Cu^{2+}, and Zn^{2+} in synthetic stormwater was studied using Visual MINTEQ 3.1. As shown in Fig. S2, at pH = 7.0 that HM exposure experiments were conducted, the majority of Pb was present in the forms of Pb^{2+} (48%), $PbSO_4$ (11%), $PbHCO_3^+$ (10%), and $PbOH^+$(9%), with no solid specie present. At this pH, the majority of Cu was found as aqueous species of Cu^{2+} (48%), $CuCO_3$ (33%), $CuOH^+$ (12%), and $CuSO_4$ (5%) (Fig. S3). Increasing the water pH to more than 8 results in the formation of $Pb(OH)_2$ (s) and $Cu(OH)_2$ (s) precipitates. At pH = 7.0, the majority of Zn was present as Zn^{2+}(88%), and it precipitates as $Zn(OH)_2$ (s) when the pH varied between 9 and 11 (Fig. S4).

3.2. Surface chemistry variation due to the photodegradation

The ATR-FTIR spectroscopy analysis revealed significant variations in LDPE MPs' surface chemistry due to the eight weeks of UV-B radiation (Fig. 1a). The major peaks in the new LDPE MPs spectra appeared as a strong doublet at 2918 cm^{-1} and 2853 cm^{-1}, which attribute to $–CH_2$ asymmetrical and symmetrical stretching vibrations. Additionally, the $–CH_2$ bending deformation and $–CH_2$ rocking deformation peaks occurred at 1468 cm^{-1} and 718 cm^{-1}, respectively, as confirmed by the literature (Bonyadinejad et al., 2022; Gulmine et al., 2003). After exposure of LDPE MPs to UV-B radiation for eight weeks, a major peak was observed at 1723 cm^{-1} representing the carbonyl group's (>C═O) formation. Additionally, the peaks were found at 1162 cm^{-1} and in the region of 3100–360 cm^{-1} correspond to > C–O< and >OH functions, respectively (Martínez-Romo et al., 2015; Babaghayou et al., 2016). The carbonyl index of photodegraded LDPE MPs (1.7) was found to be greater than that of new LDPE MPs (0.3).

3.3. Organic carbon leaching from new and photodegraded MPs

To identify the impact of organic carbon leached from the new and photodegraded LDPE MPs on their HM uptake behavior, the organic leaching experiments were conducted under similar conditions as the kinetics experiments. The results revealed a quadratic increase in DOC concentration for both new (R^2 = 0.9520) and photodegraded MPs (R^2

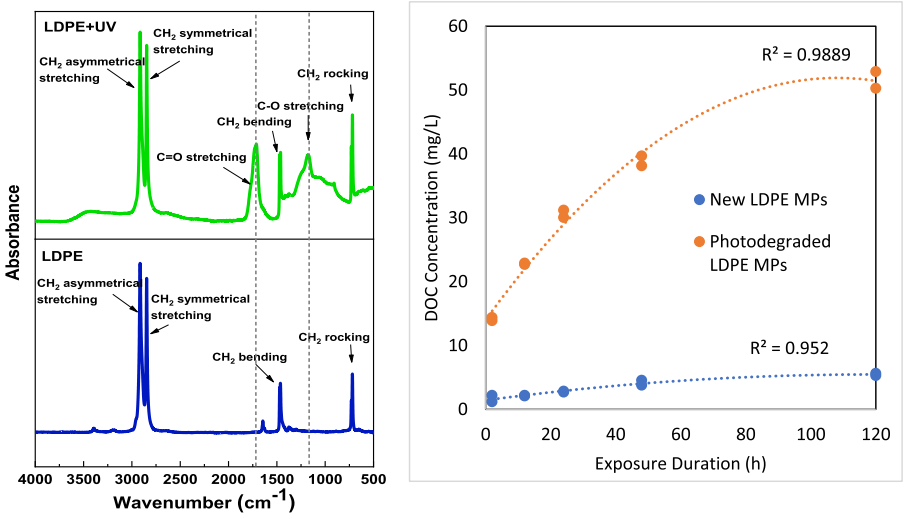

(a) (b)

Fig. 1. (a) ATR-FTIR spectra and (b) DOC leaching by new and photodegraded LDPE MPs.

= 0.9889) throughout the 120 h exposure period (Fig. 1b). However, a significantly greater concentration of DOC was released from photodegraded LDPE MPs compared to the new MPs (p-value<0.05). The average DOC concentration increased from 2.7 mg/L to 5.3 mg/L for the water contacted new LDPE MPs and from 31.2 mg/L to 52.8 mg/L for the water contacted photodegraded LDPE MPs. The dynamic condition caused by mixing may have enhanced the leaching of these dissolved organic matter from MPs to the water by increasing the concentration gradient. Unreacted monomers and oligomers leached out of the new LDPE MPs could have increased the DOC concentration over the exposure period. On the other hand, photodegradation creates the oxidized surface functional groups on the plastic surface and results in the polymeric chain scission (Bonyadinejad et al., 2022). Thus, the generated photodegradation byproducts and short polymeric chains may have leached out of the MPs into the contact water. Our findings are supported by Romera-Castillo et al. (2022), that reported more than two orders of magnitude DOC leaching from photodegraded LDPE MPs compared to new MPs (Cristina et al., 2022). Moreover, Zhu et al. (2020) reported the photo dissolution of plastics due to solar radiation and suggested that DOC is the major by-product of sunlight-induced photodegradation of plastics.

3.4. Heavy metals accumulation onto the new and photodegraded LDPE MPs

The Cu, Zn, and Pb accumulation onto the new and photodegraded LDPE MPs was studied at two intervals (6 h and 12 h) at the initial concentration of 300 μg/L and in the absence of the sediments. The new MPs showed negligible Cu, Zn, and Pb uptake (<0.1 μg/g) at both intervals. However, significantly greater levels of Cu, Zn, and Pb were accumulated onto the photodegraded LDPE MPs compared to the new MPs (p-value<0.05) (Fig. S5). The order of HMs accumulation onto the photodegraded MPs after 6 h exposure period was Pb > Cu > Zn with 9.9 μg/g of Pb, 5.6 μg/g of Cu, and 2.4 μg/g of Zn. Extending the exposure duration to 12 h did not result in a significant increase of metal loadings (p-value>0.05), suggesting that the photodegraded MPs have been saturated in the first 6 h of the exposure period and that prolonged exposure may not influence the metal loadings. The photodegradation process led to the formation of oxidized carbon surface functional groups [>C═O, >C–*O*–C<] on MPs, which may have promoted electrostatic interaction and complexation between MPs and HM species present in the aqueous solution. Moreover, surface cracks, crazes, and increased surface roughness due to photodegradation could have increased the physical confinement of the HM species onto the photodegraded MPs (Herath and Salehi, 2022; Hadiuzzaman et al., 2022; Salehi et al., 2018). BET surface area analysis revealed that the surface area of the new LDPE MPs increased from 0.8 m^2/g to 3.3 m^2/g due to the photodegradation process. Additionally, DOC leaching experiments showed the presence of 22.7 mg/L of DOC in the water that contacted the photodegraded LDPE samples for 12 h, which could have formed complexes with HMs and prevented their further accumulation onto the photodegraded MPs (Salehi et al., 2018; Weng et al., 2002). Ionic competition could explain the lower Zn and Cu uptake compared to Pb. The results suggest that the HMs' surface loading is inversely proportional to the respective hydrated ionic radius. Pb^{2+}, with the smallest hydrated ionic radius of 0.401 nm, had the highest metal uptake compared to Cu^{2+} and Zn^{2+}, with respective hydrated ionic radii of 0.419 and 0.430 nm (Hawari and Mulligan, 2007; Nightingale Jr, 1959; Zou et al., 2020). Furthermore, the electronegativity of metal ions influences their adsorption, with Pb-(2.33) exhibiting the greatest electronegativity and adsorption onto LDPE compared to Cu-(1.90) and Zn-(1.65) (Allen and Brown, 1995; Faur-Brasquet et al., 2002; Salam et al., 2012). This finding is consistent with the previous research reported greater Pb adsorption than Zn onto plastic materials in HMs mixture solutions (Aghilinasrollahabadi et al., 2021; Rochman et al., 2014).

3.5. Heavy metals adsorption by sediments

The extent of Cu, Zn, and Pb uptake by the sediments at three different sediments concentrations (200 mg/L, 400 mg/L, 600 mg/L) when MPs were absent was studied (Fig. 2). Similar to MPs, increasing the contact time from 6 h to 12 h did not affect the metal sorption capacities for all studied metals (p-value>0.05), indicating that surface saturation had occurred at 6 h. The sediments' adsorption of HMs followed a sequence of Pb, Cu > Zn, which is consistent with the results reported by Elliott et al. (1986) and corresponds to increasing the pK_a for the first hydrolysis product of each metal ion [$PbOH^+$, $CuOH^+$, $ZnOH^+$]. Although organic matters were removed from the sediments during pretreatment, the sediments contained a variety of oxide minerals with hydroxyl groups (-OH) that could donate their proton to the surrounding aqueous solution and uptake the metal ions. For instance, goethite

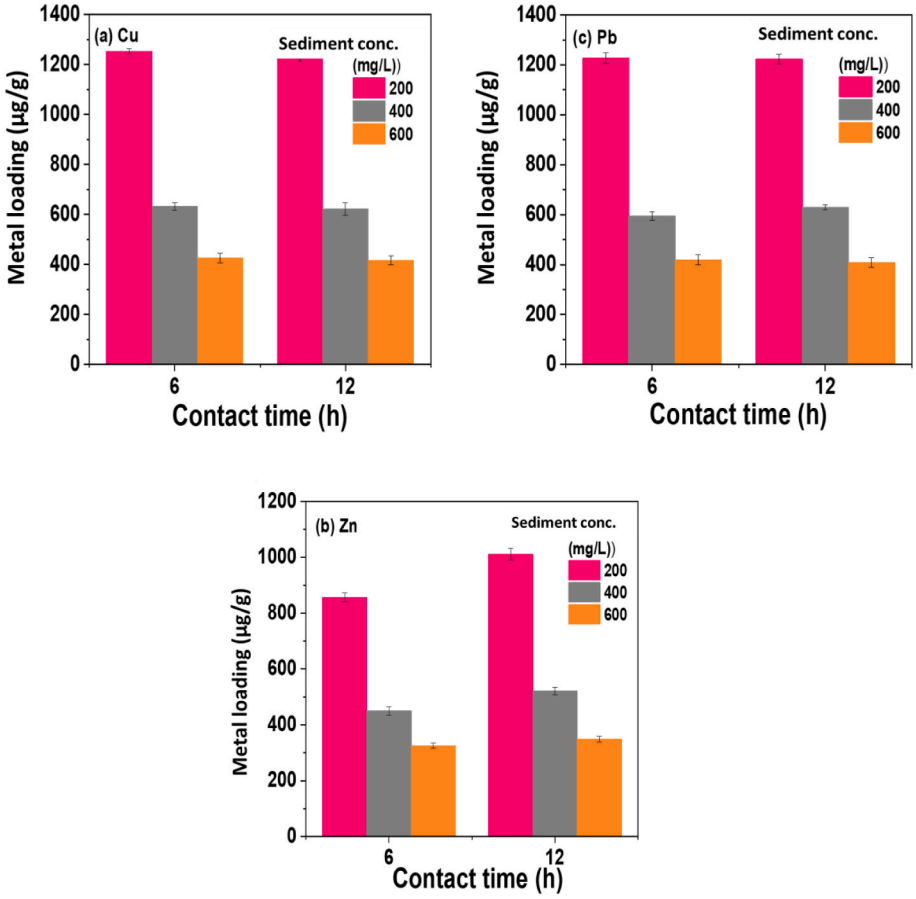

Fig. 2. (a) Cu, (b) Zn, and (c) Pb mass loadings on sediments at different time intervals at 200 mg/L, 400 mg/L, and 600 mg/L sediment concentrations ($[Cu]_t = 300$ µg/L, $[Pb]_t = 300$ µg/L, $[Zn]_t = 300$ µg/L, pH = 7.0).

(α-FeOOH) has four hydroxyls with different reactivities, and aluminosilicate contains both silanol (≡Si–OH) and aluminol (≡Al–OH) edge-surface groups (Bradl, 2004). As expected, HM loading on sediments decreased with increasing the sediment concentration as more sites became available for their accumulation. The greatest HM mass loadings on sediment particles were found at 200 mg/L of sediment concentration, with maximum Cu, Zn, and Pb mass loadings of 1228 µg/g, 1010 µg/g, and 1223 µg/g, respectively. Therefore, this sediment concentration (200 mg/L) was used for the kinetics experiments.

3.6. The kinetics of HMs partitioning between MPs and sediments

The partitioning of HMs between the MPs and sediment was studied by conducting the kinetics experiment for an aqueous system containing MPs and sediments. Results showed that Pb, Cu, and Zn adsorptions by new MPs were below detection limits during the entire exposure period, whereas HMs mass loadings on photodegraded MPs increased sharply to 21.7, 16.4, and 25.1 µg/g for Cu, Zn, and Pb, respectively, after 24 h exposure period (Fig. 3a). However, increasing the exposure duration from 24 h to 48 h, caused a decrease in the mass loadings of all target metals for photodegraded LDPE, possibly due to the release of metal ions upon prolonged periods. The percentage reductions of Cu, Zn, and Pb loadings on photodegraded MPs by increasing the metal exposure duration from 24 h to 48 h were 12.5%, 30.3%, and 26.8%, respectively. Considering the results of DOC leaching, it is worth noting that the increasing number of organic molecules released from photodegraded MPs over the exposure duration may have led to the formation of complexes with HMs present on the MPs surface, resulting in their release back into the aqueous phase (Salehi et al., 2018).

The Cu, Zn, and Pb mass loadings on sediments, after 48 h exposure period and in the presence of the new MPs were found as 484 µg/g, 1101 µg/g, and 1877 µg/g, respectively (Fig. 3b), lower than the conditions where only sediments were present within the system. However, using the mass balance approach, no detectable HMs uptake was found for sediments when they were present with the photodegraded MPs in kinetics experiments. The DOC leaching results demonstrated that a significant amount of organic carbon was leached by the photodegraded MPs into the contact water during the exposure period. Therefore, the three main components of sediment minerals, photodegraded MPs, and dissolved organic matter, competed with each other in making complexes with the HMs. From HMs uptake results, it inferred the affinity of the HMs toward sediments was reduced when photodegraded MPs were present. Based on the extent of dissolved organic carbon released from photodegraded MPs to the contact water, it can be inferred that the HMs could be associated with the DOC in the aqueous phase, as reported in the literature (Jönsson et al., 2006). Fig. 4 provides a schematic illustration of HMs uptake by new and photodegraded MPs and sediments.

First- and second-order kinetics models were applied for the metal adsorption data to identify the mechanism of HM uptake by MPs and sediments according to equations (3) and (4), where t is the contact time (h), q_e denotes the Cu, Zn, or Pb mass loading (µg/g) at the equilibrium time, q_t is metal mass loading at time t (µg/g) and k_1 and k_2 are the first- and second-order rate constants. Nonlinear forms of the first- and second order kinetics equations were used to calculate the kinetics parameters using the solver in Excel. R^2 values were calculated using equation (5), where ASSR is the sum of the squared differences between capacity average for experiment and model, and SSR is the sum of the squared differences between capacity for experiment and model. Greater R^2 values were found using the second-order kinetics model for metal uptake by both sediments and photodegraded MPs compared to the first-

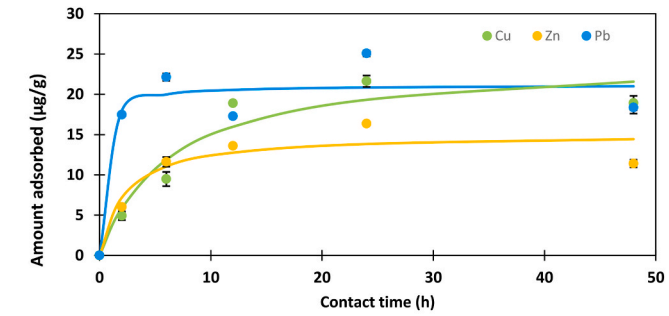

(a)

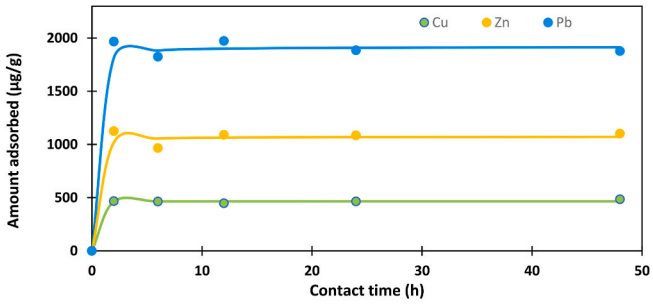

(b)

Fig. 3. Cu, Zn, and Pb mass loadings for (a) photodegraded MPs when sediments were present and (b) sediments when new MPs were present ($[Cu]_t$ = 500, $[Pb]_t$ = 500, $[Zn]_t$ = 500), pH = 7.0], and fitted second-order kinetics model.

order kinetics model in the majority of the cases, as shown in Table 2. This indicates that the rate-limiting step for metal adsorption onto photodegraded MPs and sediment mainly occurs through chemical association, which involves sharing electrons between metal cations and active sites on MPs and sediment surfaces. Several studies (Hadiuzzaman et al., 2022; Tang et al., 2021) have shown that HM accumulation onto MPs follows second-order kinetics, which involves metal complexation, coordination, and chelation. Furthermore, additional experiments were conducted to examine the rapid metal uptake by photodegraded MPs and sediments in their mixture by quantifying the metal uptake by those after 5 min, 15 min, 30 min, and 60 min exposure at conditions similar to the kinetics experiments. The results (Figure S6) showed a gradual increase in HMs uptake by photodegraded MPs when sediments were present during their early stages of HMs exposure. Moreover, some HM uptake by sediments was found during the early stages of HMs exposure ($t \leq 1$ h) when they were present with the photodegraded MPs, with its reduction over time indicating the desorption process. On the other hand, the HM uptake by sediments when new MPs were present was constantly high, which shows their very rapid metal uptake. The partitioning coefficient (K_d) was calculated by dividing the metal mass loading on MPs or sediments (µg/g) by the metal mass concentration (µg/L) in the aqueous solution at the equilibrium (24 h). Since the metal uptake on the new LDPE was very low and below the detection limits, the partition coefficient values calculated were insignificant. Partitioning coefficients for Cu, Zn, and Pb uptake on photodegraded LDPE were obtained as 0.16, 0.09, and 4.43 (L/g), respectively. Pb exhibited the highest value indicating the greater metal uptake on MPs surface compared to Cu and Zn, which is consistent with the kinetics data. The partitioning coefficients for sediments, when they were present with the new MPs, were calculated as 1.16 for Cu, 4.12 for Zn, and 23.2 (L/g) for Pb.

$$q_t = q_e\left(1 - e^{-k_1 t}\right) \quad (3)$$

$$t/q_t = t/qe + 1/k_2 q_e^2 \quad (4)$$

$$R^2 = 1 - (ASSR / SSR) \quad (5)$$

3.7. The influence of heavy metals' initial concentrations on their partitioning between microplastics and sediments

This study investigated the influence of increasing the HMs' concentrations on their partitioning between MPs and sediments. The initial concentrations of Cu, Zn, and Pb were increased from 100 µg/L to 2000 µg/L to determine the impact on the HMs accumulation onto new and photodegraded MPs and sediments. The Cu, Zn, and Pb loadings onto the new MPs were below the detection limits, regardless of the presence of

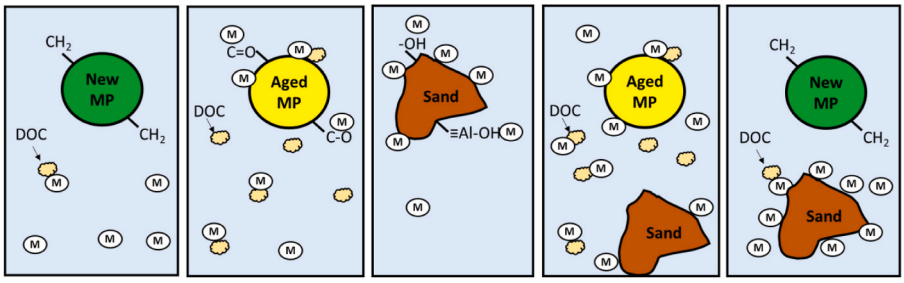

Fig. 4. Schematic demonstrating the metal uptake by new and photodegraded MPs, sediments, and a mixture of sediment, photodegraded, and new MPs.

Table 2
Kinetics parameters of Cu, Zn, and Pb accumulation on photodegraded MPs and sediments for an aqueous system containing MPs and sediments.

		Kinetics model						
			First order			Second order		
	Metal	q_e (exp.) (µg g^{-1})	q_e (cal.) (µg g^{-1})	k_1 (h^{-1})	R^2	q_e (cal.) (µg g^{-1})	k_2 (g µg^{-1} h^{-1})	R^2
Photodegraded LDPE	Cu	20.26	20.833	0.238	0.936	24.421	0.008	0.982
	Zn	13.88	13.934	0.293	0.999	15.101	0.030	0.999
	Pb	21.71	20.707	0.943	0.999	21.148	0.134	1
Sediments/New LDPE	Cu	474	465.412	4.112	0.999	465.61	0.371	1
	Zn	1093	1073.30	0.980	0.987	1073.29	0.009	0.989
	Pb	1811	1904.82	0.493	0.969	1917.29	0.005	0.972

sediments. This lower metal uptake may be attributed to the minimal diffusion of metal species to the MPs' surface sites caused by a lower electrostatic attraction and surface confinement of the HM species. However, increasing the initial HMs concentrations led to similar rates of HMs accumulation onto the photodegraded MPs in the absence and presence of the sediments (Fig. 5). In the absence of the sediments and at the initial HMs concentration of 2000 μg/L, the Cu, Zn, and Pb mass loadings on photodegraded LDPE were found as 56, 22, 103 μg/g, respectively. Although HMs' loadings were slightly greater for photodegraded LDPE in the absence of sediments, they were not significantly different from when sediments were present (p-value>0.05). The Cu (r^2 = 0.888) and Pb (r^2 = 0.941) mass loadings on photodegraded MPs were increased linearly by increasing initial metal concentrations, but the linear regression coefficient (r^2 = 0.495) was lower for Zn uptake by photodegraded MPs in the absence of the sediments. A similar trend was found for Zn and Pb uptake by photodegraded MPs in the presence of the sediments. HMs uptake by sediments in the absence or presence of new MPs increased linearly with increasing initial metal concentrations (r^2>0.99) (Fig. 6). Increasing the initial concentrations of Cu, Zn, and Pb from 100 μg/L to 2000 μg/L resulted in an increase in their mass loadings on sediments from 413 μg/g, 386 μg/g, 433 μg/g to 9971 μg/g, 9864 μg/g, 9857 μg/g, respectively. The metal loadings on sediments did not change in the presence of new MPs (p-value>0.05). However, having a mixture of sediments with photodegraded MPs lowered the sediments' metal uptake in which applying the mass balance approach revealed no significant HM uptake for the sediments. This could be due to the elevated level of organic matter leached by photodegraded MPs into the water, which may have formed complexes with HMs and prevented their accumulation onto the sediments.

Photodegraded MPs showed a greater Pb surface loading than Cu and Zn. Although all metal ions were in the divalent form, they had different affinities towards MPs. It can be observed that metal surface loading is inversely proportional to their respective hydrated ionic radius. Surface oxidation caused by UV-B photodegradation of MPs introduced oxygen-containing functionalities that are more susceptible to metal uptake through electrostatic attractions, metal complexation, and chelation (Mao et al., 2020; Li et al., 2019; Fu et al., 2021). Moreover, the alteration of MPs' physiochemical properties and an increase in surface area, polarity, and hydrophilicity facilitate HM uptake (Liu et al., 2022). However, it has been reported that an increase in solution ionic strength due to salinity could inhibit metal uptake as the counter ions strongly compete for cationic adsorption sites on MPs' surface and impede the electrostatic interactions for the HMs (Zou et al., 2020).

4. Limitations and broader implications

In this study, we excluded the impact of the sediments' organic matter content to solely elucidate the interaction of their inorganic functions with the HM species present within the stormwater runoff. However, under natural or built environmental conditions, organic matter is present within the sediment structure ranging from 0.5% to 5% (Huang and Keller, 2020). These organic matters originate from decaying plants, vegetation, organisms, and anthropogenic pollution and could form coordinated bonding with HM ions present within the stormwater runoff. Future investigation is needed to identify how different levels and types of organic matter present within the sediments impact their susceptibility to accumulate HMs while co-present with new and weathered MPs. Additionally, the biofilm presence on MPs and sediments may critically affect the HM accumulation behavior through biosorption, microbial-mediated metal transformation, and surface complexation. The metal release process should also be further investigated in addition to the metal uptake, as it will influence the bioavailability of HMs. All metal uptake experiments in this study were conducted using bivalent metal cations as they are the most common valences for Pb, Zn, and Cu found within the environment (Gledhill et al., 1997; Tang et al., 2021). Although, other possible valences such as Pb^{4+} and Cu^{1+} are only present under certain conditions [e.g., oxidizing environment] (Yeom et al., 1997; Salehi et al., 2018; Cook et al., 2012), which rarely occur within the stormwater environment. With the alteration of metal valences, different complexes form in the water, and hydrated ionic radii and charges may change. All these variations could influence the physical confinement of metallic ions onto the plastic surface sites and their electrostatic attractions. Future study is required to investigate the influence of metal valency on its adsorption behavior. Moreover, determining HMs uptake by sediments through applications of mass balance rather than directly digesting and quantifying the sediments' metal content is considered a limitation for this study as this method might not be sensitive enough to identify the small metal uptakes by the sediment. However, it clearly showed a significant reduction of HMs uptake by sediments when they were present with the photodegraded MPs in the aqueous solution compared to the condition that the photodegraded MPs were absent. Even though this study was associated with several limitations, it provided valuable information that sheds light on the important mechanisms of HM's transport by MPs present within stormwater. Notably, it demonstrated that as plastic particles age within the environment, they become susceptible to HMs uptake. On the other hand, aged plastics leach more organic matter to the contact water, creating another medium to compete with the inorganic sediments in creating complexes with the available HMs, thus limiting their sequestration within the mineral components. It could be alarming as this process facilitates the transport of HMs via stormwater runoff to adjacent water resources and might threaten aquatic lives. Moreover, as reported in the literature, most plastic-derived DOC compounds are low molecular weight organics that make them very bioavailable (Zhu et al., 2020). This is concerning as their transport via stormwater runoff to freshwater resources could perturb the activities, diversity, and composition of the microbial communities (Carlson et al., 2002).

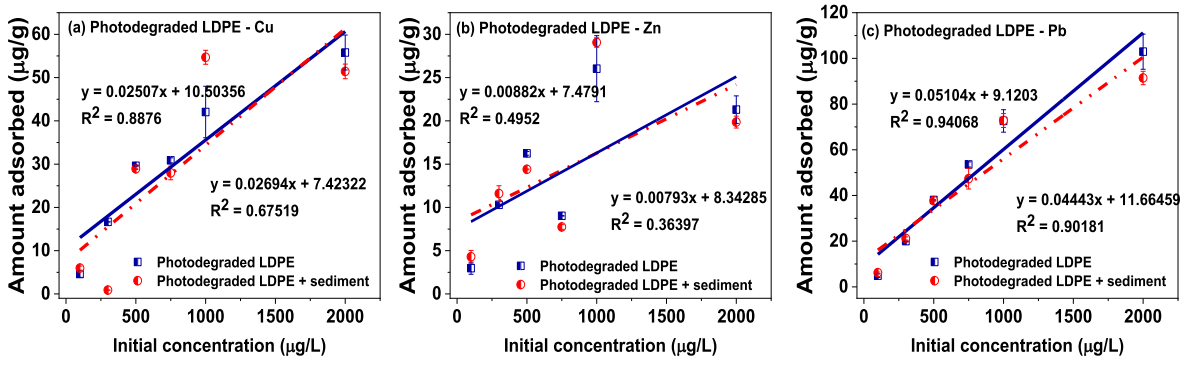

Fig. 5. Cu, Zn, and Pb mass loadings on photodegraded LDPE in the absence and presence of sediments.

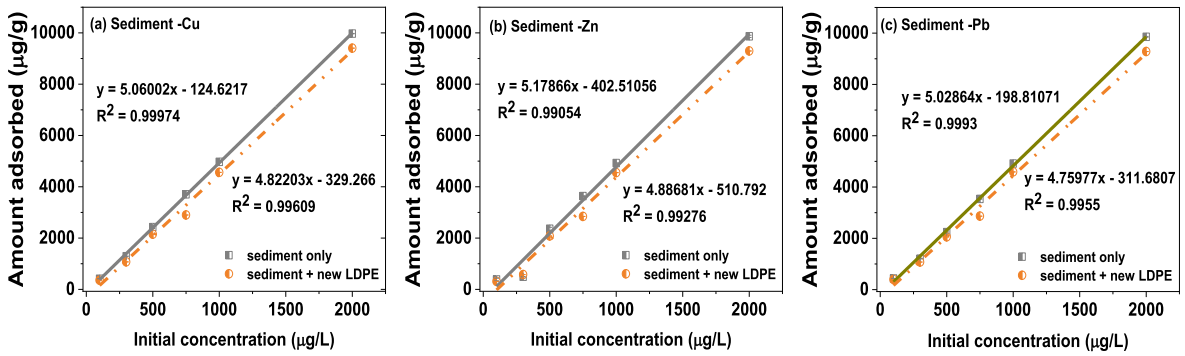

Fig. 6. Cu, Zn, and Pb mass loadings of sediments in the absence and presence of new LDPE MPs.

5. Conclusion

In this study, a systematic investigation was conducted to identify how the co-presence of new and photodegraded MPs and sediments influence the transport of HMs via stormwater runoff. For this purpose, the influence of accelerated photodegradation of LDPE MPs on their surface chemistry alterations and DOC leaching was studied, and its link to the accumulation of Cu, Zn, and Pb onto new and photodegraded MPs in the presence and absence of sediments was examined. The results revealed significant surface oxidation of MPs due to eight weeks of photodegradation and greater levels of DOC leaching compared to new MPs during the entire exposure period. Although the HMs uptake by new MPs in the absence/presence of sediments was negligible, it was significant for photodegraded MPs. The HM uptake by sediments was significantly reduced when the photodegraded MPs were present within the aqueous system. Considering the DOC leaching results, it was inferred that organic matters leached by photodegraded MPs had a greater affinity to form complexes with available HMs within the system. For most metals, the second-order kinetics model better fits the metal accumulation onto the photodegraded MPs and sediments, indicating the possible chemical association as the rate-controlling step.

Credit author statement

Amali Herath: Methodology, investigation, writing, visualization; Dibya Datta: Investigation, Gholamreza Bonyadinejad: Investigation; Maryam Salehi: Conceptualization, Methodology, Writing and Editing, Demonstration, Supervising, Funding acquisition.

Declaration of competing interest

The authors declare that they have no known competing financial interests or personal relationships that could have appeared to influence the work reported in this paper.

Data availability

Data will be made available on request.

Acknowledgment

Thanks to Dr. Tanju Karanfil from Clemson University for conducting the BET analysis. Funding for this work was provided by the United States National Science Foundation grant CBET-2044836, and the United States Department of Agriculture, National Institute of Food and Agriculture (USDA/NIFA) Award number 2020-67019-31166.

Appendix A. Supplementary data

Supplementary data to this article can be found online at https://doi.org/10.1016/j.chemosphere.2023.138844.

References

Aghilinasrollahabadi, K., Salehi, M., Fujiwara, T., 2021. Investigate the influence of microplastics weathering on their heavy metals uptake in stormwater. J. Hazard Mater. 408 https://doi.org/10.1016/j.jhazmat.2020.124439.

Ahamed, T., Brown, S.P., Salehi, M., 2020. Investigate the role of biofilm and water chemistry on lead deposition onto and release from polyethylene: an implication for potable water pipes. J. Hazard Mater. 400, 123253 https://doi.org/10.1016/j.jhazmat.2020.123253.

Allen, S.J., Brown, P.A., 1995. Isotherm analyses for single component and multi-component metal sorption onto lignite. J. Chem. Technol. Biotechnol.: International Research in Process, Environmental AND Clean Technology 62 (1), 17–24.

Babaghayou, M.I., Mourad, A.-H.I., Lorenzo, V., de la Orden, M.U., Urreaga, J.M., Chabira, S.F., Sebaa, M., 2016. Photodegradation characterization and heterogeneity evaluation of the exposed and unexposed faces of stabilized and unstabilized LDPE films. Mater. Des. 111, 279–290.

Bonyadinejad, G., Salehi, M., Herath, A., 2022. Investigating the Sustainability of Agricultural Plastic Products, Combined Influence of Polymer Characteristics and Environmental Conditions on Microplastics Aging. Science of The Total Environment, 156385.

Bradl, H.B., 2004. Adsorption of heavy metal ions on soils and soils constituents. J. Colloid Interface Sci. 277 (1), 1–18.

Carlson, C.A., Giovannoni, S.J., Hansell, D.A., Goldberg, S.J., Parsons, R., Otero, M.P., Vergin, K., Wheeler, B.R., 2002. Effect of nutrient amendments on bacterioplankton production, community structure, and DOC utilization in the northwestern Sargasso Sea. Aquat. Microb. Ecol. 30 (1), 19–36.

Cook, N.J., Ciobanu, C.L., Brugger, J., Etschmann, B., Howard, D.L., Jonge, M.D.de, Ryan, C., Paterson, D., 2012. Determination of the oxidation state of Cu in substituted Cu-In-Fe-bearing sphalerite via µ-XANES spectroscopy. Am. Mineral. 97 (2–3), 476–479.

Cristina, R.-C., Rebeca, M.-F., Marola, S.-Y., Antón, Á.-S.X., 2022. Leaching and bioavailability of dissolved organic matter from petrol-based and biodegradable plastics. Mar. Environ. Res. 176, 105607.

Elliott, H.A., Liberati, M.R., Huang, C.P., 1986. Competitive Adsorption of Heavy Metals by Soils. Wiley Online Library.

Faur-Brasquet, C., Kadirvelu, K., Le Cloirec, P., 2002. Removal of metal ions from aqueous solution by adsorption onto activated carbon cloths: adsorption competition with organic matter. Carbon 40 (13), 2387–2392.

Fiala, M., Hwang, H.-M., 2021. Influence of highway pavement on metals in road dust: a case study in Houston, Texas. Water, Air, Soil Pollut. 232 (5), 185.

Fu, Q., Tan, X., Ye, S., Ma, L., Gu, Y., Zhang, P., Chen, Q., Yang, Y., Tang, Y., 2021. Mechanism analysis of heavy metal lead captured by natural-aged microplastics. Chemosphere 270, 128624.

Gao, M., Peng, H., Xiao, L., 2021. The influence of microplastics for the transportation of E. coli using column model. Sci. Total Environ. 786, 147487.

Geyer, R., Jambeck, J.R., Law, K.L., 2017. Production, use, and fate of all plastics ever made. Sci. Adv. 3 (7), e1700782.

Gledhill, M., Nimmo, M., Brown, S.T., 1997. The toxicity of copper (II) species to marine algae, with particular reference to macroalgae. J. Phycol. 33 (1), 2–11.

Gulmine, J.V., Janissek, P.R., Heise, H.M., Akcelrud, L., 2003. Degradation profile of polyethylene after artificial accelerated weathering. Polym. Degrad. Stabil. 79 (3), 385–397.

Hadiuzzaman, M., Salehi, M., Fujiwara, T., 2022. Plastic litter fate and contaminant transport within the urban environment, photodegradation, fragmentation, and heavy metal uptake from storm runoff. Environ. Res. 212, 113183 https://doi.org/10.1016/j.envres.2022.113183.

Hawari, A.H., Mulligan, C.N., 2007. Effect of the presence of lead on the biosorption of copper, cadmium and nickel by anaerobic biomass. Process Biochem. 42 (11), 1546–1552.

Herath, A., Salehi, M., 2022. Studying the combined influence of microplastics' intrinsic and extrinsic characteristics on their weathering behavior and heavy metal transport in storm runoff. Environ. Pollut. 308, 119628.

Herngren, L., Goonetilleke, A., Ayoko, G.A., 2005. Understanding heavy metal and suspended solids relationships in urban stormwater using simulated rainfall. J. Environ. Manag. 76 (2), 149–158.
Huang, Y., Keller, A.A., 2020. Remediation of heavy metal contamination of sediments and soils using ligand-coated dense nanoparticles. PLoS One 15 (9), e0239137.
Huang, X., Zemlyanov, D.Y., Diaz-Amaya, S., Salehi, M., Stanciu, L., Whelton, A.J., 2020. Competitive heavy metal adsorption onto new and aged polyethylene under various drinking water conditions. J. Hazard Mater. 385, 121585.
Jahandari, A., 2020. Pollution status and human health risk assessments of selected heavy metals in urban dust of 16 cities in Iran. Environ. Sci. Pollut. Control Ser. 27, 23094–23107.
Jönsson, J., Sjöberg, S., Lövgren, L., 2006. Adsorption of Cu (II) to schwertmannite and goethite in presence of dissolved organic matter. Water Res. 40 (5), 969–974.
Kamali, M., Alamdari, N., Salehi Esfandarani, M., Salehi, M., 2023. Rainfall characteristics, industrial sector, total suspended solids, runoff pollutant loading characteristics, urban runoff. J. Contam. Hydrol. 256, 104179.
Kitahara, K.-I., Nakata, H., 2020. Plastic additives as tracers of microplastic sources in Japanese road dusts. Sci. Total Environ. 736, 139694.
Li, X., Mei, Q., Chen, L., Zhang, H., Dong, B., Dai, X., He, C., Zhou, J., 2019. Enhancement in adsorption potential of microplastics in sewage sludge for metal pollutants after the wastewater treatment process. Water Res. 157, 228–237.
Liu, S., Huang, J., Zhang, W., Shi, L., Yi, K., Yu, H., Zhang, C., Li, S., Li, J., 2022. Microplastics as a vehicle of heavy metals in aquatic environments: a review of adsorption factors, mechanisms, and biological effects. J. Environ. Manag. 302, 113995.
Mao, R., Lang, M., Yu, X., Wu, R., Yang, X., Guo, X., 2020. Aging mechanism of microplastics with UV irradiation and its effects on the adsorption of heavy metals. J. Hazard Mater. 393, 122515.
Martínez-Romo, A., González-Mota, R., Soto-Bernal, J.J., Rosales-Candelas, I., 2015. Investigating the degradability of HDPE, LDPE, PE-Bio, and pe-oxo films under UV-B radiation. J. Spectrosc. 2015, 1–6.
Miranda, L.S., Ayoko, G.A., Egodawatta, P., Goonetilleke, A., 2022. Adsorption-desorption behavior of heavy metals in aquatic environments: influence of sediment, water and metal ionic properties. J. Hazard Mater. 421, 126743.
Nightingale Jr., E.R., 1959. Phenomenological theory of ion solvation. Effective radii of hydrated ions. J. Phys. Chem. 63 (9), 1381–1387.
Rochman, C.M., Hentschel, B.T., Teh, S.J., 2014. Long-term sorption of metals is similar among plastic types: implications for plastic debris in aquatic environments. PLoS One 9 (1), e85433.
Rødland, E.S., Lind, O.C., Reid, M.J., Heier, L.S., Okoffo, E.D., Rauert, C., Thomas, K.V., Meland, S., 2022. Occurrence of tire and road wear particles in urban and peri-urban snowbanks, and their potential environmental implications. Sci. Total Environ. 824, 153785.
Romera-Castillo, C., Birnstiel, S., Antón Álvarez-Salgado, X., Sebastián, M., 2022. Aged plastic leaching of dissolved organic matter is two orders of magnitude higher than virgin plastic leading to a strong uplift in marine microbial activity. Front. Mar. Sci. 9, 861557.
Salam, M.A., Al-Zhrani, G., Kosa, S.A., 2012. Simultaneous removal of copper (II), lead (II), zinc (II) and cadmium (II) from aqueous solutions by multi-walled carbon nanotubes. Compt. Rendus Chem. 15 (5), 398–408.
Salehi, M., Jafvert, C.T., Howarter, J.A., Whelton, A.J., 2018. Investigation of the factors that influence lead accumulation onto polyethylene: implication for potable water plumbing pipes. J. Hazard Mater. 347, 242–251.
Salehi, M., Aghilinasrollahabadi, K., Salehi Esfandarani, M., 2020. An investigation of stormwater quality variation within an industry sector using the self-reported data collected under the stormwater monitoring program. Water 12 (11), 3185.
Scott, J.W., Gunderson, K.G., Green, L.A., Rediske, R.R., Steinman, A.D., 2021. Perfluoroalkylated substances (Pfas) associated with microplastics in a lake environment. Toxics 9 (5), 106.
Tang, S., Lin, L., Wang, X., Yu, A., Sun, X., 2021. Interfacial interactions between collected nylon microplastics and three divalent metal ions (Cu (II), Ni (II), Zn (II)) in aqueous solutions. J. Hazard Mater. 403, 123548.
Weng, L., Temminghoff, E.J.M., Lofts, S., Tipping, E., Van Riemsdijk, W.H., 2002. Complexation with dissolved organic matter and solubility control of heavy metals in a sandy soil. Environ. Sci. Technol. 36 (22), 4804–4810.
Werbowski, L.M., Gilbreath, A.N., Munno, K., Zhu, X., Grbic, J., Wu, T., Sutton, R., Sedlak, M.D., Deshpande, A.D., Rochman, C.M., 2021. Urban stormwater runoff: a major pathway for anthropogenic particles, black rubbery fragments, and other types of microplastics to urban receiving waters. ACS ES&T Water 1 (6), 1420–1428.
Yeom, Y.H., Kim, Y., Seff, K., 1997. Crystal structure of zeolite X exchanged with Pb (II) at pH 6.0 and dehydrated:(Pb4+) 14 (Pb2+) 18 (Pb4O4) 8Si100Al92O384. J. Phys. Chem. B 101 (27), 5314–5318.
Zhang, K., Hamidian, A.H., Tubić, A., Zhang, Y., Fang, J.K.H., Wu, C., Lam, P.K.S., 2021. Understanding plastic degradation and microplastic formation in the environment: a review. Environ. Pollut. 274, 116554.
Zhu, L., Zhao, S., Bittar, T.B., Stubbins, A., Li, D., 2020. Photochemical dissolution of buoyant microplastics to dissolved organic carbon: rates and microbial impacts. J. Hazard Mater. 383, 121065.
Zou, J., Liu, X., Zhang, D., Yuan, X., 2020. Adsorption of three bivalent metals by four chemical distinct microplastics. Chemosphere 248, 126064.